EurJIC
European Journal of Inorganic Chemistry

Research Article
doi.org/10.1002/ejic.202500174

Chemistry Europe
European Chemical Societies Publishing

www.eurjic.org

Reactivity of an *Ortho*-Phenylene-Bridged Al/P Frustrated Lewis Pair toward Small Molecules

Melina E. A. Dilanas and Frank Breher*

Dedicated to Prof. Dr. Werner Uhl

Frustrated Lewis pairs (FLPs) as ambiphilic molecules are prone to activate small molecules and are in the focus of interest for many years. Herein, the first *ortho*-phenylene-bridged Al/P-based FLP with only one phosphine moiety is presented. The title compound is employed in various reactions with small molecules featuring different functional groups. The Al/P-based FLP readily forms adducts or activation products and can reversibly activate CO_2 at room temperature.

1. Introduction

Frustrated Lewis pairs (FLPs) consist of a Lewis acid and Lewis base, which are geometrically hindered from forming a Lewis pair.[1–3] There are three common types of FLPs: intermolecular, intramolecular, and so-called "masked" FLPs. The intermolecular FLPs consist of a bulky Lewis acid and base, which prevent Lewis pair formation, whereas the intramolecular FLPs are restrained by a rigid linker between the reactive entities. "Masked" or "hidden" FLPs clearly form a Lewis pair and still exhibit the typical FLP-like reactivity toward small molecules and distinct organic substrates, and in some cases also allow transition metal-free catalysis.[4,5] Several review articles about FLPs, their characteristics, and reactivities appeared in recent years.[4–9]

Among the first examples of FLPs was a *p*-phenylene-bridged B/P FLP published in 2006 by Stephan et al. which was employed in metal-free hydrogenation of imines a year later. It was also shown that it stoichiometrically reduces benzaldehyde at room temperature.[10,11] Even before that, the synthesis and reactivity of *o*-phenylene-bridged aminoboranes toward HCl and H_2O resulting in zwitterionic compounds were reported by Roesler, Piers, and Parvez.[12]

In 2006, Miqueu and Bourissou et al. published the first *o*-phenylene-bridged B/P-based FLPs.[13] These scaffolds have been thoroughly employed in transition metal complexation.[13–19]

Tris(2-diphenylphosphino)phenyl aluminum (TDPA, **Scheme 1**) is synthesized via metathesis from *o*-Li-$C_6H_4PPh_2$ and $AlCl_3$.[15,20] While it was originally employed as a ligand system, Fontaine et al. investigated the reactivity of TDPA in detail. They found that TDPA displays reversible activation of CO_2 at room temperature, where complete conversion back to TDPA occurs after placing the activation product under N_2 atmosphere for 12 h. The catalytic reduction of CO_2 using TDPA as precatalyst and HBCat as hydride source was found to be possible due to an aluminum–boron exchange yielding the catalytically active B/P-FLP (cf., Scheme 1).[21] Furthermore, *mono o*-phenylene-bridged group 14 element/P compounds were published with Si, Ge, Sn, and Pb by Wesemann and Mitzel.[22–24] So far, only *o*-phenylene-bridged Al/P FLPs with more than one phosphine substituent have been described.[25] We hereby present the synthesis and characterization of a *mono o*-phenylene-bridged Al/P FLP.

2. Results and Discussion

2.1. Synthesis and Quantum Chemical Calculations

The title compound **1** was synthesized by reacting $^tBu_2AlBr$ with *o*-Li-$C_6H_4PPh_2 \cdot n\ OEt_2$ ($1.1 < n < 1.4$) following a slightly altered literature procedure (**Scheme 2**).[20] Instead of heating the reaction mixture, we found that **1** can also be synthesized at room temperature. Since the reaction in toluene always resulted in a mixture of various compounds bearing a phosphine moiety visible in $^{31}P\{^1H\}$ NMR spectroscopy, the solvent was switched to hexane. To remove traces of the formerly coordinating diethyl ether, the solvent was distilled in vacuo from the reaction mixture at 100 °C and the resulting colorless solid was extracted with hexane and filtered.

The crystallization was initiated by slowly removing the solvent at low pressure. **1** is obtained in the form of clear, colorless crystals in 82% yield. The crystal structure (space group $P2_1/n$; **Figure 1**) displays angles of ∠(P1—C2—C1) = 108.6° and ∠(C2—C1—Al1) = 108.0°, which are small compared to the ideal angle of 120° for an sp^2-hybridized carbon atom. The sum of the covalent radii of aluminum and phosphorus equals

M. E. A. Dilanas, F. Breher
Institute of Inorganic Chemistry
Karlsruhe Institute of Technology (KIT)
Engesserstr. 15, 76131 Karlsruhe, Germany
E-mail: breher@kit.edu

Supporting information for this article is available on the WWW under https://doi.org/10.1002/ejic.202500174

Research Article
doi.org/10.1002/ejic.202500174

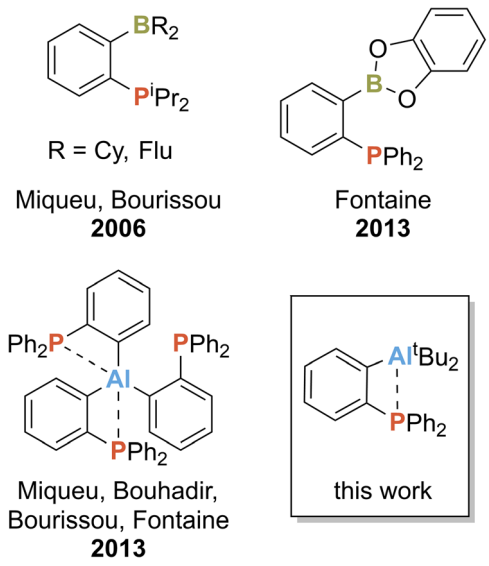

Scheme 1. Overview over some already published *o*-phenylene-bridged group 13/P FLPs. Flu, fluorenyl.

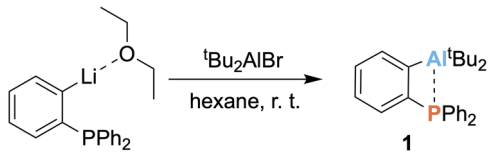

Scheme 2. Synthesis of **1**.

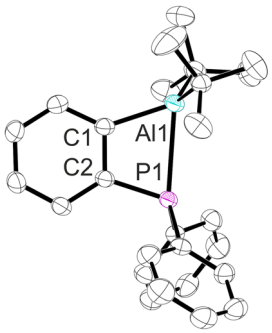

Figure 1. Molecular structure of **1**. Thermal ellipsoids are shown with a 30% probability. The hydrogen atoms are omited for clarity. Selected bond lengths (Å) and angles (°): P1—Al1 = 2.6076(7), Al1—C1 = 1.991(2), P1—C2 = 1.807(2); Al1—P1—C2 = 75.30(6), C1—Al1—P1 = 67.98(6), P1—C1—C2 = 108.62(14), C2—C1—Al1 = 107.95(15).

2.37 Å.[26] Therefore, the P1—Al1 bond of **1** (2.6076(7) Å) is longer by 0.22 Å, which is an expected result of the steric strain on the phenylene moiety. It is 8 pm shorter than the ones between aluminum and the two coordinating phosphine moieties in TDPA (2.69 Å).[20] The phosphorus carbon bonds of ≈1.80 Å all are in the same range. Also, all Al—C bonds show the expected bond lengths with values close to 2.00 Å, again corresponding to the bond lengths in TDPA (cf., Scheme 1).[20]

Calculations at the RI-PBE0-D3(BJ)/def2-TZVP level of theory implied that the HOMO−1 and HOMO−2 as well as LUMO+6 are the orbitals involved for the reactivity of **1** (**Figure 2**). The Natural Bond Orbital (NBO) analysis shows that aluminum and phosphorus can interact less with each other than in the corresponding intermolecular Lewis pair Ph_3P–Al^{t}Bu$_2$Ph (**q1**; **Table 1**). In comparison with free Ph_3P and free ^{t}Bu$_2$AlPh, the phosphorus gains and the aluminum loses positive charges due to their interactions in **1** and **q1**. Since there is less steric strain on the Al–P interaction in **q1**, the charge at P is found more positive and at Al more negative than in **1**.

The Wiberg Bond Indices (WBI) show a lower bond order between aluminum and phosphorus in **1** than in the intermolecular Lewis pair **q1**, what would be expected due to the steric strain employed by the phenylene backbone. Compared to the covalently bonded derivative Ph_2P–Al^{t}Bu$_2$ (**q2**), with additional double bond contribution, the bond order is significantly lower. Atoms in molecules (AIM) calculations (Table 1 and Figure S41, Supporting Information) depict a clear interaction between aluminum and phosphorus in **1**. The atomic charges are 2.026 e for Al and 1.303 e for P, respectively. They are comparable to the values found for **q1**. In summary, all calculations show a close resemblance between **q1** and **1** rather than **q2**.

To analyze the Al–P interaction in **1** a little further, the Ortho Interaction Energy (OIE) was calculated by determining the reaction enthalpy of a pseudo-isodesmic reaction forming the FLP, which equals the OIE (**Scheme 3**). The OIE of **1** was calculated following the method of Mitzel et al. and could be determined to be as little as −0.32 kJ mol^{-1}.[24] This is a first hint to the weak interaction between aluminum and phosphorus in **1** enabling reactivity toward small molecules.

For **q1** also, the Al–P interaction energy (AIP-E) was calculated (**Scheme 4**) to amount to −41.21 kJ mol^{-1}.

2.2. Reactivity toward Small Molecules

To explore the reactivity of **1**, we performed various reactions with small molecules. Toward CO and H_2, no reactivity was observed. Stoichiometric addition of methanol to a solution of **1** yielded quantitative decomposition to triphenyl phosphine and other unidentified compounds, regardless of the reaction being performed at room temperature or at −78 °C.

2.2.1. Reactivity toward N_2O

1 was placed in a flask and dissolved in toluene. After degassing the colorless solution 3 times via Freeze–Pump–Thaw method, 1.1 bar of N_2O was added. The colorless solution was stirred overnight, and the solvent was evaporated under low pressure until the product **2** crystallized in form of colorless blocks (space group $P2_1/n$; **Figure 3**). **2** was found to be the oxidized FLP **1** with a P═O bond length of 1.5290(15) Å corresponding to literature values.[27] The observed bond length between Al1 and O1 (1.8715(15) Å) lies in the typical range of Al—O single bonds, clearly showing a Lewis pair being formed between Al1 and O1, further saturating the electronic demand of the Lewis acidic aluminum.[26] The ν(P═O) double bond vibration was found at 1438 cm^{-1}, which matches the frequency for Ph_3P═O signifying the comparable chemical vicinity.[28] The $^{31}P\{^1H\}$ NMR chemical shift is detected at $\delta_{31P} = 50.43$ ppm in C_6D_6. The

Research Article
doi.org/10.1002/ejic.202500174

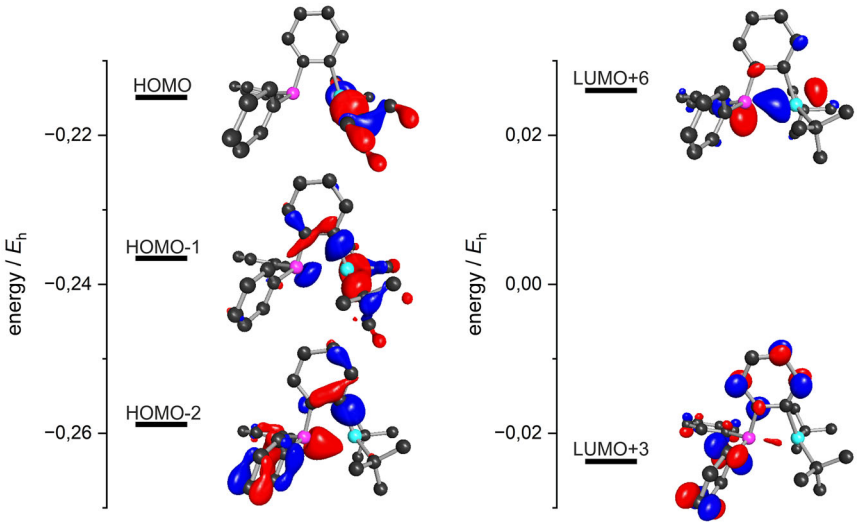

Figure 2. Kohn–Sham molecular orbitals of **1** (RI-PBE0-D3(BJ)/def2-TZVP, isosurface value of 0.05).

Table 1. NBO analyses,[85] atoms in molecules charges,[86–88] and WBI[89] of **1**, Ph_3P–Al$^tBu_2$Ph (**q1**), Ph_2P–Al$^tBu_2$ (**q2**), PPh_3, and $^tBu_2$AlPh (RI-PBE0-D3(BJ)/def2-TZVP).

Molecule	NBO		AIM		WBI
	P	Al	P	Al	Al–P
1	0.89296	1.71683	1.303666	2.026152	0.60616
q1	0.91657	1.71300	1.310965	2.028339	0.62163
q2	0.12598	1.72857	0.288429	1.945129	0.98671
PPh_3	0.82169	–	2.026152	–	–
$^tBu_2$AlPh	–	1.93032	–	2.043755	–

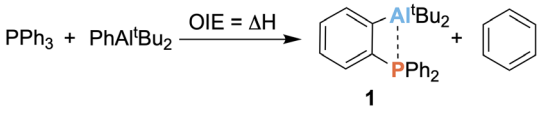

Scheme 3. Pseudo-isodesmic reaction for the calculation of the OIE of **1**.

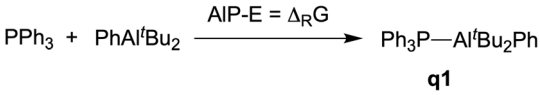

Scheme 4. Pseudo-isodesmic reaction to calculate the Al–P interaction energy of **q1**.

signal of free Ph_3PO appears at $\delta_{31P} = 29.3$ ppm, which is significantly shifted to lower frequencies.[29] A possible reason for this is the electron withdrawing aluminum atom, which forms a Lewis pair with the oxygen atom leaving it partially positively charged.

2.2.2. Reactivity toward NH_3

Gassing of a solution of **1** in toluene with 1.1 bar of NH_3 gas after degassing it 3 times with the Freeze–Pump–Traw method

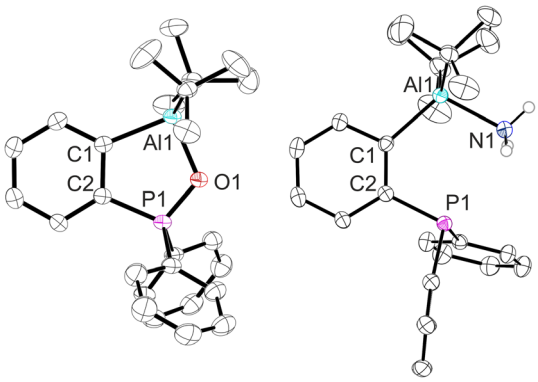

Figure 3. Molecular structures of **2** and **3**. Thermal ellipsoids are shown with a 30% probability. The hydrogen atoms (except for coordinated NH_3) are omitted for clarity. Selected bond lengths (Å) and angles (°): **2**: C1—C2 = 1.411(3), Al1—C1 = 2.017(2), Al1—O1 = 1.8715(15), P1—C2 = 1.787(2), P1—O1 = 1.5290(15); P1—C2—C1 = 112.31(17), C2—C1—Al1 = 113.50(17), C1—Al1—O1 = 90.62(8), C2—P1—O1 = 106.69(9), Al1—O1—P1 = 116.80(9). **3**: Al1—C1 = 2.0219(19), P1—C2 = 1.827(2), Al1—N1 = 2.0055(18), C1—C2 = 1.412(3); C1—Al1—N1 = 110.39(8), C2—C1—Al1 = 132.56(14), C1—C2—P1 = 117.27(13).

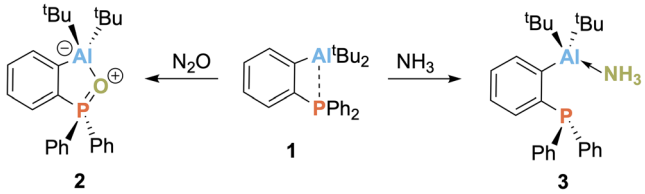

Scheme 5. Reaction of **1** with N_2O forming the oxidized species **2** and with NH_3 forming the Lewis pair **3**.

resulted in a low-frequency-shifted signal at $\delta_{31P} = -3.60$ ppm (cf., $\delta_{31P} = 1.61$ ppm for **1**). This signal belongs to the Al/N Lewis pair **3** (**Scheme 5**); the molecular structure is shown in Figure 3. Compared to **1**, the ∠(C2—C1—Al1) angle is opened to 132°, which is 12° larger than the ideal C(sp^2) angle. A possible

Research Article
doi.org/10.1002/ejic.202500174

reason for this effect is the avoidance of repulsion between the ammonia and phosphine moieties. The Al1—N1 bond length of 2.0055(18) Å is in the ranges observed for other ammonia adducts of FLPs in the literature.[30]

In contrast to another Al-based FLP recently published by our group,[31] **3** does not activate NH_3 at temperatures up to 60 °C. Furthermore, no transfer NH_3 to benzocyclobutanone could be observed at room temperature. Instead, the previously coordinated ammonia is released and **1** undergoes different reactions, which finally lead to decomposition.

2.2.3. Reactivity toward Azides

Dissolving **1** in toluene and adding a stoichiometric amount of the respective azide resulted in an instantaneous formation of the phosphazenes **4**–**6** shown in **Scheme 6**.

With trimethylsilyl azide ($TMSN_3$), N_2 was formed during the immediately occurring reaction. A colorless, five-membered AlC_2PN ring compound **4** is formed (Scheme 6). Typically, harsh reaction conditions such as temperatures >200 °C have to be employed for FLPs to release N_2 during or after the reaction with azides, which is why this reactivity is extraordinary.[32–34]

The molecular structure of **4** is depicted in **Figure 4**. The P1—N1 bond lengths of 1.6124(18) Å are indicative for a P=N double bond corresponding to typical phosphazene P=N bond lengths.[35,36] All other respective bond lengths of **4** are comparable to azide activation products by FLPs in the literature.[34]

The $^{31}P\{^1H\}$ NMR shift is detected at $\delta_{31P} = 35.76$ ppm and the ν(P=N) vibration is visible at 1019 cm^{-1} for **4**, which corresponds well with the literature values.[37]

Only $TMSN_3$ undergoes this kind of reactivity with **1**. Once larger substituents are introduced at the azide moiety, no gas formation was observed. The reactions of **1** with phenyl and mesityl azide (PhN_3 or $MesN_3$) gave five-membered ring compounds with a exocyclic azide moiety (cf., Scheme 6). There are various examples in the literature for the activation of azides by Al/P FLPs resulting in the same arrangement of Lewis base, nitrogen atoms, and Lewis acid.[34,38,39]

The molecular structures of **5** and **6** are shown in Figure 4. The N1—N2 bond lengths of 1.3816(13) and 1.3726(11) Å for **5** and **6**, respectively, are in line with a single bond; the ones for N2—N3 resemble elongated double bonds (1.2562(14) Å for **5** and 1.2619(12) Å for **6**). These bond lengths are similar to a reaction product of an ethylene-bridged B/P-based FLP with PhN_3[33,40] and a variety of differently substituted geminal FLPs.[39]

The structures were also confirmed by IR spectroscopy, where the N1—N2 single and N2=N3 double bonds are visible at 1101 and 1084 cm^{-1} as well as 1436 and 1436 cm^{-1} for **5** and **6**, respectively. The $^{31}P\{^1H\}$ NMR shifts of $\delta_{31P} = 31.41$ ppm (**5**) and $\delta_{31P} = 29.89$ ppm (**6**) show a slightly different shift compared to the $TMSN_3$ activation product **4** (cf., $\delta_{31P} = 35.76$ ppm). This can be an effect of less electron density being withdrawn from the phosphorus atom, which corresponds to the slightly longer bond between P1 and N1 in **5** and **6** as compared to **4**.

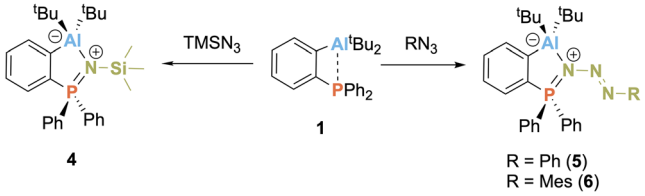

Scheme 6. Reactivity of **1** toward RN_3 forming compounds **4**, **5**, and **6**.

2.2.4. Reactivity toward PhNCO and PhNCS

The reactivity toward PhNCO was observed as expected for FLPs (**Scheme 7**).[6,27,34,38,40–43] After adding PhNCO at room temperature to a solution of **1** in toluene, a clear pale-yellow solution

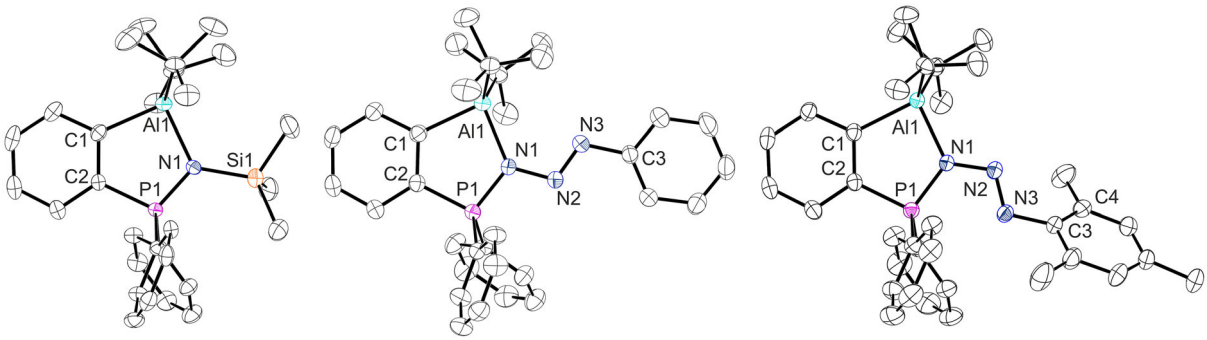

Figure 4. Molecular structures of **4**, **5**, and **6**. Thermal ellipsoids are shown with a 30% probability. The hydrogen atoms are omitted for clarity. Selected bond lengths (Å) and angles (°): **4**: C1—Al1 = 2.015(2), C2—P1 = 1.791(2), Al1—N1 = 1.9794(19), P1—N1 = 1.6124(18), N1—Si1 = 1.7871(19); Al1—C1—C2 = 113.99(15), P1—C2—C1 = 115.36(15), Al1—N1—P1 = 112.46(10), C1—Al1—N1 = 91.55(8), Al1—N1—Si1 = 124.72(10), C2—P1—N1 = 106.54(10), P1—N1—Si1 = 121.62(11). **5**: C1—Al1 = 2.0184(13), C2—P1 = 1.7897(12), Al1—N1 = 1.9572(10), P1—N1 = 1.6427(10), N1—N2 = 1.3816(13), N2—N3 = 1.2562(14), N3—C3 = 1.4303(15); Al1—C1—C2 = 116.83(9), P1—C2—C1 = 115.56(9), Al1—N1—P1 = 118.52(5), C1—Al1—N1 = 87.37(5), Al1—N1—N2 = 127.48(7), C2—P1—N1 = 101.46(5), P1—N1—N2 = 112.88(7), N1—N2—N3 = 110.13(9), N2—N3—C3 = 113.32(10). **6**:[a] C1—Al1 = 2.0091(10), C2—P1 = 1.7975(10), Al1—N1 = 1.9576(8), P1—N1 = 1.6719(8), N1—N2 = 1.3726(11), N2—N3 = 1.2619(12), N3—C3 = 1.4347(12); Al1—C1—C2 = 115.91(7), P1—C2—C1 = 117.00(7), Al1—N1—P1 = 117.65(4), C1—Al1—N1 = 88.74(4), Al1—N1—N2 = 123.85(6), C2—P1—N1 = 100.68(4), P1—N1—N2 = 118.23(6), N1—N2—N3 = 112.28(8), N2—N3—C3 = 116.07(8), N2—N3—C3—C4 = 44.91(4). [a] The solvent molecule, which cocrystallized half in the asymmetric unit was omitted for clarity.

Research Article
doi.org/10.1002/ejic.202500174

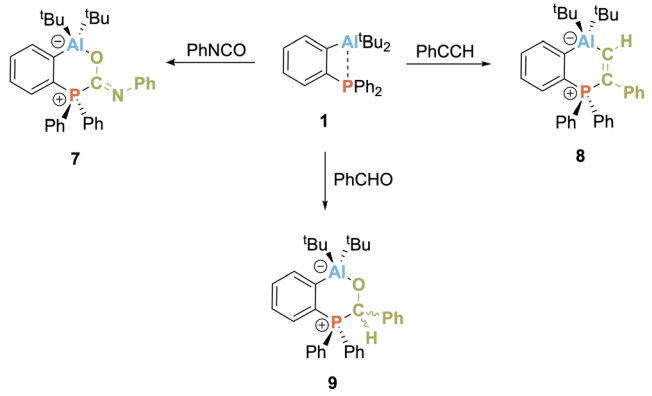

Scheme 7. Reactivity of **1** toward PhNCO, PhCCH, and PhCHO resulting in compounds **7**, **8**, and **9**.

was formed. Evaporation of the solvent and recrystallization from toluene yielded **7** as yellow crystals (space group $P-1$).

The O1—C1 bond length of 1.281(4) Å was found to be rather short for a single bond, whereas the C1—N1 bond length resembles the ideal imine bond length of 1.27 Å, also visible in the activation product of phenyl isocyanate by a geminal Al/P FLP in the literature.[44]

The $^{31}P\{^{1}H\}$ NMR shift of $\delta_{31P} = -2.67$ ppm is shifted to lower frequencies as compared to **1**. The detected chemical shift is comparable to the one observed for **3** (cf., $\delta_{31P} = -3.60$ ppm), where also another Lewis base (NH_3) is binding to the aluminum atom. The strong IR stretching vibration at 1625 cm^{-1} corresponds to ν(C=N), which is comparable to a PhNCO activation product in the literature.[47] The ν(C—O) vibration is visible at 1104 cm^{-1}, signifying the single bond character between C1 and O1.

Reaction of **1** toward PhNCS furnished a yellow solution, and the NMR spectra indicate a quantitative reaction with a new $^{31}P\{^{1}H\}$ NMR chemical shift at $\delta_{31P} = 9.42$ ppm. This compound then over time either decomposes or rearranges to show a new $^{31}P\{^{1}H\}$ NMR chemical shift at $\delta_{31P} = 2.35$ ppm. So far, we were not able to identify the product.

2.2.5. Reactivity toward Phenylacetylene

The reaction of **1** with PhCCH results in a clear solution at room temperature. The literature suggests that phenylacetylene can be deprotonated by an FLP, which results in a protonated Lewis basic moiety and leaves the acetylene moiety bound to the Lewis acidic center. At high temperatures, the C—C triple bond might be activated.[45,46]

NMR data of the reaction of **1** with PhCCH show a reaction product, which can be identified by the strongly shifted doublet at $\delta_{1H} = 9.07$ ppm with a coupling constant of $^{3}J_{HP} = 58.2$ Hz in the ^{1}H NMR spectrum corresponding to an activated triple bond with the proton in *trans*-position to the phosphorus atom.[30] The $^{31}P\{^{1}H\}$ NMR chemical shift is observed at $\delta_{31P} = 2.42$ ppm. A ^{31}P-^{1}H-2D NMR spectrum confirmed the coupling between those two signals, further validating the hypothesis of activation of phenylacetylene by **1** forming compound **8** (Scheme 7). The reaction is occurring, yet very slowly, at room temperature and takes up to 15 days to reach a conversion of 90%. The deprotonation of phenylacetylene was not observed. Unfortunately, no single crystals of **8** could be obtained; however, the product was fully characterized (see Experimental Part for details).

2.2.6. Reactivity toward Benzaldehyde

With benzaldehyde, the typical FLP-type reactivity was observed.[11,47] The oxygen atom binds to the aluminum atom and the aldehydic carbon atom forms a bond to the phosphorus atom of the FLP. Since a stereogenic center is generated, compound **9** is formed in a racemic mixture, which crystallizes in the monoclinic space group $P2_1$.

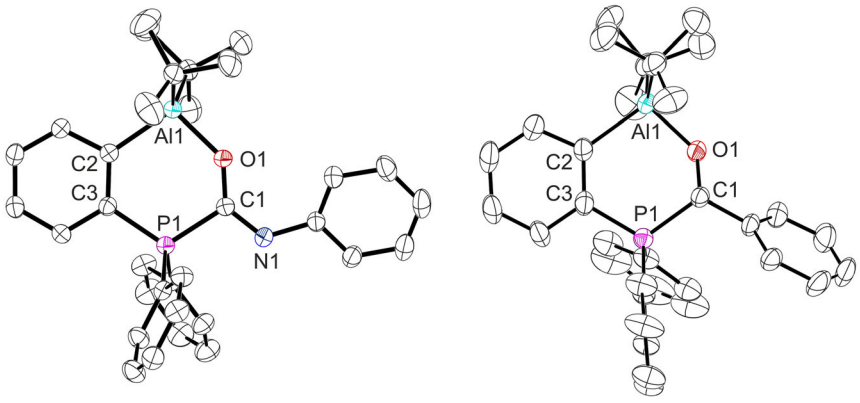

Figure 5. Molecular structures of **7** and **9**. Thermal ellipsoids are shown with a 30% probability. The hydrogen atoms are omitted for clarity. Selected bond lengths (Å) and angles (°) for **7**:[a] Al1—C2 = 2.004(3), Al1—O1 = 1.821(2), P1—C3 = 1.805(3), P1—C1 = 1.859(3), C2—C3 = 1.386(4), O1—C1 = 1.281(4), C1—N1 = 1.273(4); P1—C3—C2 = 121.9(2), C3—C2—Al1 = 126.7(2), C2—Al1—O1 = 101.73(12), Al1—O1—C1 = 134.1(2), C3—P1—C1 = 113.07(14), P1—C1—O1 = 120.7(2), O1—C1—N1 = 131.6(3), P1—C1—N1 = 107.6(2). **9**:[b] Al1—C2 = 2.034(4), Al1—O1 = 1.797(3), P1—C3 = 1.796(4), P1—C1 = 1.887(4), C1—O1 = 1.370(4); Al1—C2—C3 = 125.1(3), P1—C3—C2 = 121.0(3), C2—Al1—O1 = 100.88(15), Al1—O1—C1 = 125.4(3), P1—C1—O1 = 108.6(3), C3—P1—C1 = 110.51(17). [a] A second molecule of **7** in the asymmetric unit was omitted for clarity. The bond lengths differ slightly (<5 pm) between both molecules (see Supporting Information for complete list). [b] For clarity, only the *S*-configured molecule is shown.

Research Article
doi.org/10.1002/ejic.202500174

The molecular structure of **9** is depicted in **Figure 5**. The P1—C1 bond displays a bond length of 1.887(4) Å, which lies in the range of typical bond lengths (i.e., 1.86 Å) and is comparable to the PhNCO activation product **7**.[26] The Al1—O1 bond length of 1.797(3) Å in contrast lies below the respective one in **7** (1.821(2) Å). Given that the C—O bond of the activation product **7** is longer by nearly 0.10 Å, it appears that the activation of the aldehyde is stronger and, therefore, the bond order between C1 and O1 is more reduced.

The structure was also confirmed by IR spectroscopy through the ν(C—O) vibration. The latter was detected at 1109 cm^{-1} corresponding to the one for **7**, which was found at 1104 cm^{-1}. This is again in agreement with a single bond between C1 and O1 and, therefore, the activation of benzaldehyde.

2.2.7. Reactivity toward SO_2

After degassing of a solution of **1** in benzene-d_6 via Freeze–Pump–Thaw method 3 times, 1.1 bar of SO_2 was added. An orange solution was formed instantly. Unfortunately, decomposition of the reaction product prevented full characterization of the resulting compound. ^1H and $^{31}P\{^1H\}$ NMR spectra could be obtained once, quickly, without decomposition and could unfortunately not be reproduced. The $^{31}P\{^1H\}$ NMR signal of this activation product was observed at $\delta_{31P} = -2.15$ ppm, which is shifted to lower frequencies as compared to **1**.

2.2.8. Reactivity toward CO_2

A solution of **1** in toluene was degassed 3 times via Freeze–Pump–Thaw method and afterward gassed with 1.1 bar CO_2. At room temperature, decomposition was observed. At −78 °C, however, **1** cleanly reacted with CO_2 without decomposition. On small scale, the formerly colorless solution of **1** turned yellow during the reaction with CO_2. On larger scale, the solution turned deep yellow at low temperatures as well and turned nearly colorless as it warmed up to room temperature, which indicated a different reaction product. As the solvent was evaporated under low pressure, the pale-yellow solution turned deep yellow again. Recrystallization from toluene yielded yellow crystals of **10** (space group $P-1$; **Scheme 8**). The crystal structure shown in **Figure 6** displays the activation product of CO_2 with an additional equivalent of **1** coordinating via the aluminum atom to the terminal oxygen atom.

Multiple crystallization attempts of the colorless reaction product **11** failed, such as layering different solvents, slow evaporation of the solvent, or cooling a concentrated solution. A successful attempt was performed by gassing a saturated solution of **1** in hexane, which resulted in the instantaneous formation of a colorless solid in a yellow solution. From earlier experiments it was already known that **11** dissolves badly in hexane, which is why this solvent was chosen for the crystallization attempt. Overnight, one single large colorless crystal formed, which crystallized in the monoclinic space group $P2_1/c$ and could be

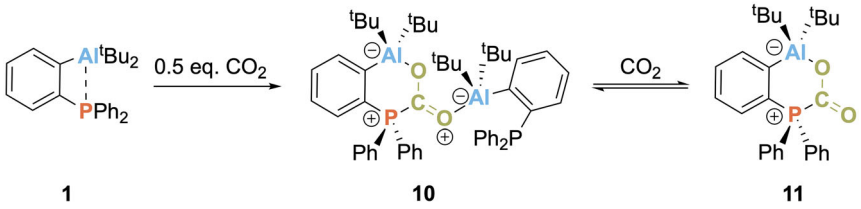

Scheme 8. Reactivity of **1** toward CO_2 forming compound **10** with 0.5 equivalents of CO_2 and compound **11** with 1 equivalent of CO_2. The coordination of **1**–**10** is reversible upon addition of CO_2 in excess.

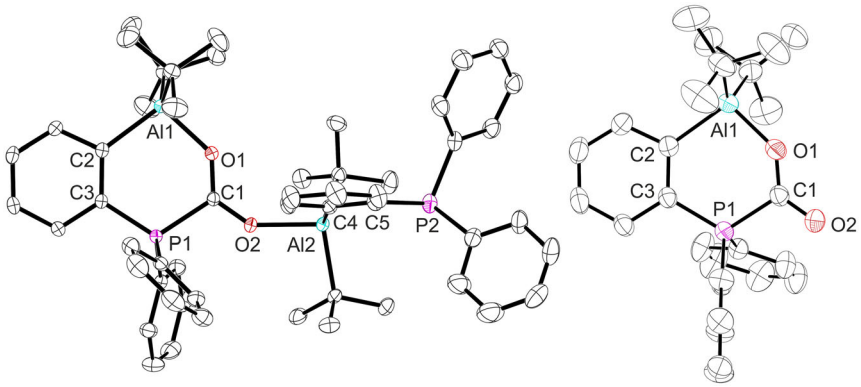

Figure 6. Molecular structures of **10** (left) and **11** (right) Thermal ellipsoids are shown with a 30% probability. The hydrogen atoms are omitted for clarity. Selected bond lengths (Å) and angles: **10**: P2—Al2 = 3.3584(5), Al1—C2 = 2.0053(12), Al2—C4 = 2.0155(12), Al1—O1 = 1.8891(9), Al2—O2 = 1.9685(8), P1—C3 = 1.7787(12), P2—C5 = 1.8267(13), P1—C1 = 1.8801(11), O1—C1 = 1.2456(13), O2—C1 = 1.2441(13); P1—C3—C2 = 121.79(8), C3—C2—Al1 = 127.32(8), C2—Al1—O1 = 100.50(4), Al1—O1—C1 = 134.77(7), Al2—O1—C1 = 144.30(8), C3—P1—C1 = 113.33(5), P1—C1—O1 = 121.19(8), P1—C1—O2 = 111.58(8), O1—C1—O2 = 127.21(10), O2—Al2—C4 = 96.62(4), Al2—C4—C5 = 123.74(9), C4—C5—P2 = 116.76(9). **11**: Al1—C2 = 2.0105(14), Al1—O1 = 1.8415(12), P1—C3 = 1.7885(13), P1—C1 = 1.8873(14), O1—C1 = 1.2594(18), O2—C1 = 1.2025(17); P1—C3—C2 = 119.67(10), C3—C2—Al1 = 126.44(10), C2—Al1—O1 = 101.44(6), Al1—O1—C1 = 135.51(10), C3—P1—C1 = 113.97(6), P1—C1—O1 = 118.54(10), P1—C1—O2 = 113.72(11), O1—C1—O2 = 127.73(13).

Research Article
doi.org/10.1002/ejic.202500174

analyzed by single-crystal X-ray diffraction. Over the course of 30 min, the colorless solid turned bright yellow under argon atmosphere. **11** seems to be only stable under CO_2 atmosphere and decomposes to **10** and CO_2 as soon as the atmosphere is changed to inert gas. In the perfluoropolyalkylether oil used for crystal picking in comparison, the compound appears to be stable for longer time periods.

The Al1—O1 bond length in **10** resembles the expected length of an Al—O single bond, being 1.8891(9) Å, whereas the Al2—O2 bond length is longer by 8 pm.[26] The bond angles ∠(Al1—C2—C3) = 127° and ∠(C2—C3—P1) = 122° are slightly larger than typical aromatic C(sp^2) bond angles of 120°. These angles probably are a result of the heteroatoms included in the six membered ring. A slight bending of the phosphine moiety of P2 toward the coordinating Al2 is possible, explaining the bond angle of 117° instead of 120° at ∠(C4—C5—P2). In general, all here observed bond lengths and angles resemble those in the literature.[20]

In **11**, the Al1—O1 bond is about 5 pm shorter than in **10**, what corresponds to the 2 pm shorter O1—C1 bond length in **11**, too. The terminal double bond between C1 and O2, which is only 4 pm shorter in **11** than in **10**, shows the little alteration by to the coordination of another molecule of **1**. All phosphorus carbon bond lengths only differ by less than 3 pm, which is why they can be regarded uninfluenced by the reaction.

The bond angles ∠(C—C—E) at the bridging carbon atoms C2 and C3 increase significantly when going from **1** to the reaction products **10** or **11**. The bond angles ∠(C2—C3—P1) in **10** and **11** are very close to the ideal angle of 120°, whereas the angles ∠(C3—C2—Al1) show higher values of 127° for **10**° and 126° for **11**, respectively. Between **10** and **11**, only small changes in the bond angles of less than 3° occur.

IR spectroscopy shows the ν(C=O) vibration of **11** at 1639 cm^{-1}, corresponding to the literature.[48]

According to calculations, the activation of CO_2 to form compound **11** is exergonic by 6.48 kJ mol^{-1} (RI-PBE0-D3(BJ)/def2-TZVP). The subsequent coordination of a second equivalent of **1** to form **10** is exergonic by another 7.23 kJ mol^{-1}, resulting in a total Gibbs free reaction enthalpy of 13.72 kJ mol^{-1}.

To analyze the nonstorable **11** a little further, a reaction of **10** with an excess of CO_2 was performed in a J. Young NMR tube. As expected, after degassing twice and then applying 1.1 bar of CO_2, the solution turned almost colorless (formation of **11**). The NMR spectrum verified the reaction with only one signal present in the $^{31}P\{^1H\}$ NMR spectrum at $\delta_{31P} = -7.68$ ppm (**Figure 7**B). The reversibility of the CO_2 activation was further investigated by removing all volatile components in vacuo (Figure 7C). During this process, NMR spectra were measured after every color change to follow the transition between **10** and **11**. As mentioned above, the colorless solution shows only one ^{31}P NMR signal at $\delta_{31P} = -7.68$ ppm. As soon as the color changed to yellow during the process of applying vacuum, two NMR chemical shifts are present at $\delta_{31P} = -0.45$ and -6.39 ppm (Figure 7C), indicating a fast equilibrium (**10** ⇌ **11**) on the NMR time scale. After complete evaporation of the solvent, both signals are further shifted to higher frequencies ($\delta_{31P} = 0.03$ and -4.34 ppm; Figure 7D). Although the chemical shifts are not exactly congruent to the starting point, it appears reasonable to assume that compound **10** is formed during the process of evacuation. We note in passing that this process can be repeated multiple times without decomposition.

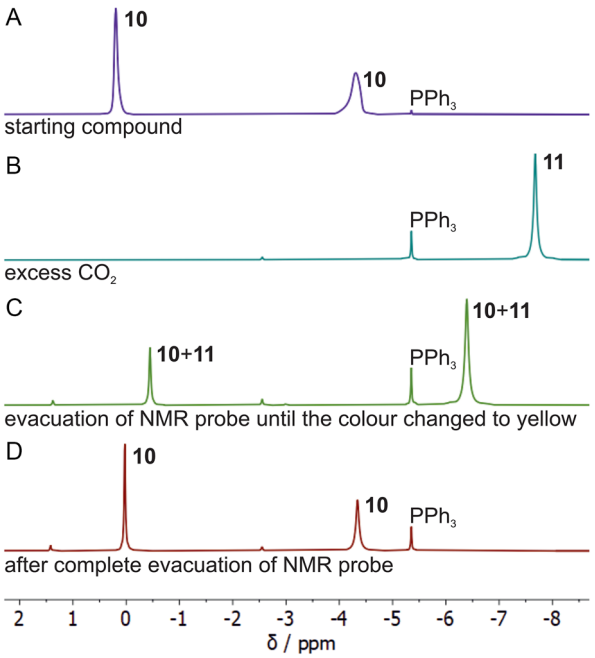

Figure 7. $^{31}P\{^1H\}$ NMR spectra of **10** after gassing with excess CO_2 and following evacuation—**A**: starting compound **10**; **B**: gassing with excess CO_2; **C**: partial evacuation of the NMR probe; **D**: after complete evacuation of the NMR probe. PPh_3 occurs due to partial decomposition of **10** by reaction with water of the slightly impure CO_2 gas.

In view of the full reversibility of the process described above, we envisaged a catalytic CO_2 reduction and transfer. This was tested by adding 2 mol% of **1** to a J. Young NMR tube, dissolving it in C_6D_6 and adding 50 equivalents of pinacol borane (HBPin).[20] The mixture was degassed 3 times via Freeze–Pump–Thaw method, and 1.1 bar CO_2 was added. At room temperature, the conversion rate was very slow, which is why the mixture was heated to 60 °C for several days with continuous NMR spectroscopic monitoring. Only after 10 days, a beginning transition of HBPin to MeO-BPin and PinB-O-BPin is visible. This unusual behavior of a very long induction period made us wonder whether some by-products

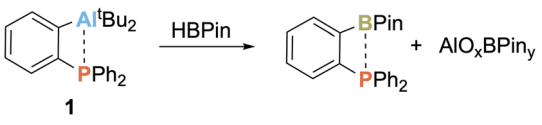

Scheme 9. Reaction of **1** with HBPin (Pin = pinacol).

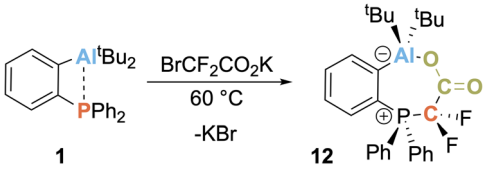

Scheme 10. Reaction of **1** with $BrCF_2CO_2K$.

Research Article
doi.org/10.1002/ejic.202500174

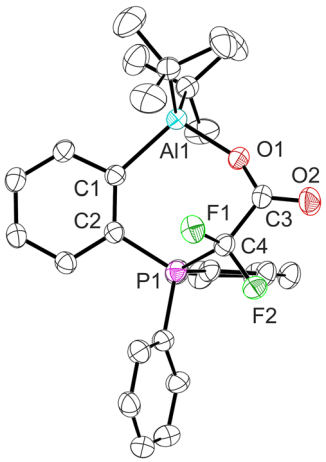

Figure 8. Molecular structure of **12**. Thermal ellipsoids are shown with a 30% probability. The half molecule of benzene in the asymmetric unit and the hydrogen atoms are omitted for clarity. Selected bond lengths (Å) and angles: C1—C2 = 1.401(4), C1—Al1 = 2.045(3), C2—P1 = 1.790(3), Al1—O1 = 1.823(2), P1—C4 = 1.886(3), O1—C3 = 1.258(4), C3—O2 = 1.205(4), C3—C4 = 1.548(4); C2—C1—Al1 = 133.6(2), C1—C2—P1 = 121.3(2), Al1—O1—C3 = 148.4(2), O1—C3—C4 = 115.2(3), C3—C4—P1 = 117.7(2).

that may arise under these conditions are responsible for the catalysis. Fontaine et al. suggested an Al—B exchange resulting in the catalytically active *ortho*-borylated phosphine as mechanism for the occurring activation of CO_2.[20,21] By having a closer look to the $^{31}P\{^1H\}$ NMR spectra, we indeed observed the formation of the *ortho*-borylated phosphine with an NMR chemical shift at $\delta_{31P} = -3.94$ ppm too. Based on a targeted synthesis of *o*–(BPin)$C_6H_4PPh_2$ following a literature procedure, this NMR chemical shift was confirmed.[49]

With this knowledge, **1** and HBPin were mixed in a J. Young NMR tube to initiate the Al—B exchange on purpose. After 21 days, quantitative conversion of **1** to *o*–(BPin)$C_6H_4PPh_2$ and small amounts of PPh_3 had occurred (**Scheme 9**). CO_2 was added to the reaction mixture and NMR spectra indicated an instantaneous start of the catalytic activity supporting the hypothesis of Al—B exchange being responsible for the catalytic activity.

2.2.9. Reactivity toward $BrCF_2CO_2K$

$BrCF_2CO_2K$ can be employed as a carbene precursor by formation of CO_2 and KBr during the reaction.[50,51] The reaction of **1** with $BrCF_2CO_2K$ commences already at room temperature, where a triplet at $\delta_{31P} = 31.76$ ppm is observable in the ^{31}P NMR spectrum. After heating the sample up to 60 °C overnight, the corresponding doublet at $\delta_{19F} = -94.05$ ppm is visible in the ^{19}F NMR spectrum, both featuring a coupling constant of 89 Hz. Corresponding single-crystal X-ray diffraction data showed the formation of compound **12** (**Scheme 10**). As highlighted by the atom coloring in the schematic drawing, **12** can be regarded as an CO_2 activation product of an *ortho*-metalated phosphorus ylide, similar to the compounds previously published by our group.[31,52,53]

12 crystallizes in the triclinic space group *P*—1 with half a molecule of benzene in the asymmetric unit; the molecular structure is shown in **Figure 8**. The bond lengths and angles all correspond to the previously published CO_2 activation product, where the fluorine atoms of **12** are methyl moieties instead.[52]

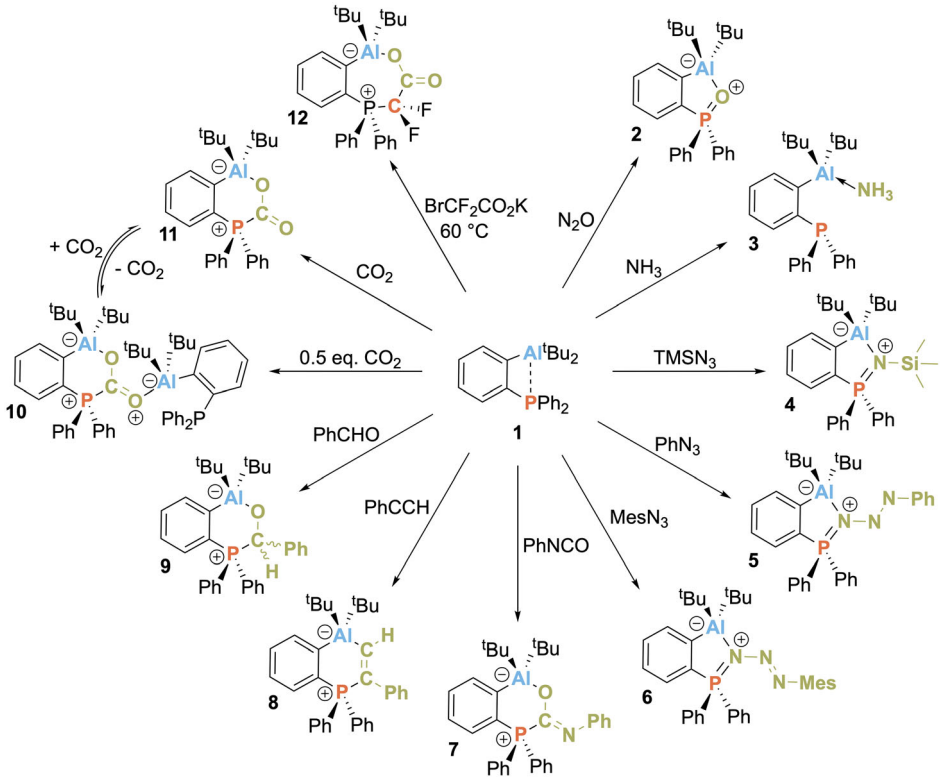

Scheme 11. Overview over the isolated and characterized compounds derived from **1**.

The CO_2 vibration can be found at 1736 cm^{-1}. Interestingly, the ν(C=O) stretching frequencies of the previously published CO_2 activation products were located between 1657 and 1683 cm^{-1}, depending on the substituents bound to Al,[52] which is significantly lower than the found frequency for **12**. This signifies the influence of the fluorine atoms on the ylidic carbon atom (**Scheme 11**).

3. Conclusion

The first *mono o*-phenylene bridged Al/P-based FLP **1** and its reactivity toward various small molecules was presented. As depicted in Scheme 10, several typical FLP-type reactivities were found, such as the formation of **5**, **6** (azide activation products), **7** (PhNCO activation product), or **9** (benzaldehyde activation product). Reaction of **1** with NH_3 provided the adduct **3**, not undergoing an N—H activation at temperatures up to 60 °C. With $TMSN_3$, **1** undergoes a rather uncommon reaction by instantaneously releasing N_2 furnishing the reaction product **4**. Most interestingly, the activation of CO_2 is reversible at room temperature making it possible to switch between the yellow compound **10** and the colorless compound **11**. The reaction of **1** with KCO_2CF_2Br leads to an incorporation of the CO_2CF_2 moiety between the aluminum and phosphorus atoms providing **12**, which can be regarded as CO_2 activation product of an ylide-based Al/C FLP previously described by our group.[31,52,53] This might be a suitable entry point for generating other Al/C-based FLPs starting from the Al/P compound **1**.

Acknowledgements

The authors acknowledge support by the German Research Foundation (DFG) through grant no. BR 2169/5-1 (535548579). Support by the state of Baden-Württemberg through bwHPC and the German Research Foundation (DFG) through grant no. INST 40/575-1 FUGG (JUSTUS 2 cluster) is also acknowledged. The authors acknowledge the Studienstiftung des Deutschen Volkes e.V. for financial support of this work in form of a doctoral scholarship for M.E.A. Dilanas. This work was partly carried out with the support of the Karlsruhe Nano Micro Facility (KNMF), a Helmholtz Research Infrastructure at Karlsruhe Institute of Technology (KIT), and the authors thank Prof. Dieter Fenske and Dr. Olaf Fuhr for their help with XRD. The research group of PD Dr. Alexander Hinz is acknowledged for providing the azides.

Conflict of Interest

The authors declare no conflict of interest.

Data Availability Statement

The data that support the findings of this study are available in the supplementary material of this article.

Keywords: aluminum · ambiphilic molecules · bond activation · frustrated Lewis pairs · phosphorus

[1] G. N. Lewis, *J. Am. Chem. Soc.* **1916**, *38*, 762.
[2] G. N. Lewis, *Valence and the Structure of Atoms and Molecules*, Chemical Catalog Co, New York **1923**.
[3] J. S. J. McCahill, G. C. Welch, D. W. Stephan, *Angew. Chem. Int. Ed.* **2007**, *46*, 4968.
[4] D. W. Stephan, G. Erker, *Angew. Chem. Int. Ed.* **2015**, *54*, 6400.
[5] D. W. Stephan, G. Erker, *Chem. Sci* **2014**, *5*, 2625.
[6] D. W. Stephan, G. Erker, *Angew. Chem. Int. Ed.* **2010**, *49*, 46.
[7] D. W. Stephan, *Science* **2016**, *354*, 1248.
[8] D. W. Stephan, *Acc. Chem. Res.* **2015**, *48*, 306.
[9] D. W. Stephan, *J. Am. Chem. Soc.* **2015**, *137*, 10018.
[10] G. C. Welch, R. R. San Juan, J. D. Masuda, D. W. Stephan, *Science* **2006**, *314*, 1124.
[11] P. A. Chase, G. C. Welch, T. Jurca, D. W. Stephan, *Angew. Chem. Int. Ed.* **2007**, *46*, 8050.
[12] R. Roesler, W. E. Piers, M. Parvez, *J. Organomet. Chem.* **2003**, *680*, 218.
[13] S. Bontemps, G. Bouhadir, K. Miqueu, D. Bourissou, *J. Am. Chem. Soc.* **2006**, *128*, 12056.
[14] M. Sircoglou, G. Bouhadir, N. Saffon, K. Miqueu, D. Bourissou, *Organometallics* **2008**, *27*, 1675.
[15] M. Sircoglou, N. Saffon, K. Miqueu, G. Bouhadir, D. Bourissou, *Organometallics* **2013**, *32*, 6780.
[16] A. Amgoune, D. Bourissou, *Chem. Commun.* **2011**, *47*, 859.
[17] J. Fajardo, J. C. Peters, *Inorg. Chem.* **2021**, *60*, 1220.
[18] B. E. Cowie, F. A. Tsao, D. J. H. Emslie, *Angew. Chem. Int. Ed.* **2015**, *54*, 2165.
[19] I. Kuzu, I. Krummenacher, J. Meyer, F. Armbruster, F. Breher, *Dalton Trans.* **2008**, 5836.
[20] M.-A. Courtemanche, J. Larouche, M.-A. Légaré, W. Bi, L. Maron, F.-G. Fontaine, *Organometallics* **2013**, *32*, 6804.
[21] M.-A. Courtemanche, M.-A. Légaré, L. Maron, F.-G. Fontaine, *J. Am. Chem. Soc.* **2013**, *135*, 9326.
[22] S. Freitag, K. M. Krebs, J. Henning, J. Hirdler, H. Schubert, L. Wesemann, *Organometallics* **2013**, *32*, 6785.
[23] J. Schneider, K. M. Krebs, S. Freitag, K. Eichele, H. Schubert, L. Wesemann, *Chem. Eur. J.* **2016**, *22*, 9812.
[24] L. Wickemeyer, J. Schwabedissen, P. C. Trapp, B. Neumann, H.-G. Stammler, N. W. Mitzel, *Dalton Trans.* **2023**, *52*, 2611.
[25] F. Krämer, *Angew. Chem. Int. Ed. Engl.* **2024**, *63*, e202405207.
[26] P. Pyykkö, M. Atsumi, *Chemistry* **2009**, *15*, 186.
[27] X. Xu, G. Kehr, C. G. Daniliuc, G. Erker, *J. Am. Chem. Soc.* **2013**, *135*, 6465.
[28] P. Linstrom, NIST Chemistry WebBook, NIST Standard Reference Database 69. Triphenylphosphine oxide, National Institute of Standards and Technology, **1997**.
[29] T. A. Albright, W. J. Freeman, E. E. Schweizer, *J. Org. Chem.* **1975**, *40*, 3437.
[30] C. Appelt, J. C. Slootweg, K. Lammertsma, W. Uhl, *Angew. Chem. Int. Ed.* **2013**, *52*, 4256.
[31] F. Krämer, J. Paradies, I. Fernández, F. Breher, *Nat. Chem.* **2024**, *16*, 63.
[32] M. W. P. Bebbington, S. Bontemps, G. Bouhadir, D. Bourissou, *Angew. Chem. Int. Ed.* **2007**, *46*, 3333.
[33] A. Stute, L. Heletta, R. Fröhlich, C. G. Daniliuc, G. Kehr, G. Erker, *Chem. Commun.* **2012**, *48*, 11739.
[34] D. Pleschka, M. Layh, F. Rogel, W. Uhl, *Philos. Trans. A. Math. Phys. Eng. Sci.* **2017**, *375*, 20170011.
[35] L. Zhu, R. Kinjo, *Chem. Soc. Rev.* **2023**, *52*, 5563.
[36] J. Backs, M. Lange, J. Possart, A. Wollschläger, C. Mück-Lichtenfeld, W. Uhl, *Angew. Chem. Int. Ed.* **2017**, *56*, 3094.
[37] H. Schmidbaur, W. Wolfsberger, *Chem. Ber.* **1967**, *100*, 1016.
[38] L. Keweloh, H. Klöcker, E.-U. Würthwein, W. Uhl, *Angew. Chem. Int. Ed.* **2016**, *55*, 3212.
[39] W. Uhl, J. Backs, A. Hepp, L. Keweloh, M. Layh, D. Pleschka, J. Possart, A. Wollschläger, *Z. Naturforsch. B* **2017**, *72*, 821.
[40] C. M. Mömming, G. Kehr, B. Wibbeling, R. Fröhlich, G. Erker, *Dalton Trans.* **2010**, *39*, 7556.
[41] J. Li, B. Li, R. Liu, L. Jiang, H. Zhu, H. W. Roesky, S. Dutta, D. Koley, W. Liu, Q. Ye, *Chem. Eur. J.* **2016**, *22*, 14499.
[42] S. Roters, C. Appelt, H. Westenberg, A. Hepp, J. C. Slootweg, K. Lammertsma, W. Uhl, *Dalton Trans.* **2012**, *41*, 9033.
[43] A. Stute, G. Kehr, R. Fröhlich, G. Erker, *Chem. Commun.* **2011**, *47*, 4288.
[44] P. Pyykkö, M. Atsumi, *Chemistry* **2009**, *15*, 12770.

[45] C. Appelt, H. Westenberg, F. Bertini, A. W. Ehlers, J. C. Slootweg, K. Lammertsma, W. Uhl, *Angew. Chem. Int. Ed.* **2011**, *50*, 3925.
[46] M. A. Dureen, D. W. Stephan, *J. Am. Chem. Soc.* **2010**, *132*, 13559.
[47] C. M. Mömming, S. Frömel, G. Kehr, R. Fröhlich, S. Grimme, G. Erker, *J. Am. Chem. Soc.* **2009**, *131*, 12280.
[48] W. Uhl, C. Appelt, *Organometallics* **2013**, *32*, 5008.
[49] K. Fukuda, T. Harada, N. Iwasawa, J. Takaya, *Dalton Trans.* **2022**, *51*, 7035.
[50] V. O. Smirnov, A. D. Volodin, A. A. Korlyukov, A. D. Dilman, *Angew. Chem. Int. Ed. Engl.* **2020**, *59*, 12428.
[51] J. Zheng, J. Cai, J.-H. Lin, Y. Guo, J.-C. Xiao, *Chem. Commun.* **2013**, *49*, 7513.
[52] F. Krämer, J. Paradies, I. Fernández, F. Breher, *Chem. Eur. J.* **2024**, *30*, e202303380.
[53] D. González-Pinardo, F. Krämer, F. Breher, I. Fernández, *ChemistryEurope* **2024**, *2*, e202400020.
[54] R. Ahlrichs, M. Bär, M. Häser, H. Horn, C. Kölmel, *Chem. Phys. Lett.* **1989**, *162*, 165.
[55] S. G. Balasubramani, G. P. Chen, S. Coriani, M. Diedenhofen, M. S. Frank, Y. J. Franzke, F. Furche, R. Grotjahn, M. E. Harding, C. Hättig, A. Hellweg, B. Helmich-Paris, C. Holzer, U. Huniar, M. Kaupp, A. Marefat Khah, S. Karbalaei Khani, T. Müller, F. Mack, B. D. Nguyen, S. M. Parker, E. Perlt, D. Rappoport, K. Reiter, S. Roy, M. Rückert, G. Schmitz, M. Sierka, E. Tapavicza, D. P. Tew, C. van Wüllen, V. K. Voora, F. Weigend, A. Wodyński, J. M. Yu, *J. Chem. Phys.* **2020**, *152*, 184107.
[56] K. Eichkorn, O. Treutler, H. Öhm, M. Häser, R. Ahlrichs, *Chem. Phys. Lett.* **1995**, *242*, 652.
[57] K. Eichkorn, F. Weigend, O. Treutler, R. Ahlrichs, *Theor. Chem. Acc.* **1997**, *97*, 119.
[58] C. Adamo, V. Barone, *J. Chem. Phys.* **1999**, *110*, 6158.
[59] M. Bursch, J.-M. Mewes, A. Hansen, S. Grimme, *Angew. Chem. Int. Ed.* **2022**, *61*, e202205735.
[60] L. Goerigk, S. Grimme, *Phys. Chem. Chem. Phys.* **2011**, *13*, 6670.
[61] D. Rappoport, N. R. M. Crawford, F. Furche, K. Burke, in *Encyclopedia of Inorganic and Bioinorganic Chemistry* (Hrsg.: R. A. Scott), John Wiley & Sons, Ltd, Chichester, UK **2011**.
[62] F. Weigend, R. Ahlrichs, *Phys. Chem. Chem. Phys.* **2005**, *7*, 3297.
[63] F. Weigend, *Physical chemistry chemical physics : PCCP* **2006**, *8*, 1057.
[64] S. Grimme, S. Ehrlich, L. Goerigk, *J. Comput. Chem.* **2011**, *32*, 1456.
[65] A. D. Becke, E. R. Johnson, *J. Chem. Phys.* **2005**, *123*, 154101.
[66] E. R. Johnson, A. D. Becke, *J. Chem. Phys.* **2005**, *123*, 24101.
[67] E. R. Johnson, A. D. Becke, *J. Chem. Phys.* **2006**, *124*, 174104.
[68] O. Treutler, R. Ahlrichs, *J. Chem. Phys.* **1995**, *102*, 346.
[69] C. Steffen, K. Thomas, U. Huniar, A. Hellweg, O. Rubner, A. Schroer, *J. Comput. Chem.* **2010**, *31*, 2967.
[70] P. Deglmann, K. May, F. Furche, R. Ahlrichs, *Chem. Phys. Lett.* **2004**, *384*, 103.
[71] M. K. Kesharwani, B. Brauer, J. M. L. Martin, *J. Phys. Chem. A* **2015**, *119*, 1701.
[72] A. Klamt, C. Moya, J. Palomar, *J. Chem. Theory Comput.* **2015**, *11*, 4220.
[73] A. Klamt, G. Schüürmann, *J. Chem. Soc., Perkin Trans. 2* **1993**, 799.
[74] F. Eckert, A. Klamt, *AIChE J.* **2002**, *48*, 369.
[75] A. Klamt, V. Jonas, T. Bürger, J. C. W. Lohrenz, *J. Phys. Chem. A* **1998**, *102*, 5074.
[76] A. S. Brown, P. M. Levin, E. W. Abrahamson, *J. Chem. Phys.* **1951**, *19*, 1226.
[77] I. Krossing, H. Nöth, S. Staude, *Z. Naturforsch. B* **2008**, *63*, 1045.
[78] S. Harder, L. Brandsma, J. A. Kanters, A. Duisenberg, J. H. van Lenthe, *J. Organomet. Chem.* **1991**, *420*, 143.
[79] J. Koziskova, F. Hahn, J. Richter, J. Kožíšek, *Acta Chim. Slovaca* **2016**, *9*, 136.
[80] O. V. Dolomanov, L. J. Bourhis, R. J. Gildea, J. A. K. Howard, H. Puschmann, *J. Appl. Crystallogr.* **2009**, *42*, 339.
[81] G. M. Sheldrick, *Acta Crystallogr. A* **2015**, *71*, 3.
[82] G. M. Sheldrick, *Acta Crystallogr. A* **2008**, *64*, 112.
[83] S. Sinnecker, A. Rajendran, A. Klamt, M. Diedenhofen, F. Neese, *J. Phys. Chem. A* **2006**, *110*, 2235.
[84] K. Barral, A. D. Moorhouse, J. E. Moses, *Org. Lett.* **2007**, *9*, 1809.
[85] A. E. Reed, R. B. Weinstock, F. Weinhold, *J. Chem. Phys.* **1985**, *83*, 735.
[86] R. F. W. Bader, *Acc. Chem. Res.* **1985**, *18*, 9.
[87] T. Lu, *J. Chem. Phys.* **2024**, *161*, 82503.
[88] T. Lu, F. Chen, *J. Comput. Chem.* **2012**, *33*, 580.
[89] K. B. Wiberg, *Tetrahedron* **1968**, *24*, 1083.

Manuscript received: April 3, 2025
Revised manuscript received: April 17, 2025
Version of record online: May 6, 2025